Effect of winter wind variability on plankton transport over Georges Bank[☆]

Craig V.W. Lewis[a,*], Changsheng Chen[b], Cabell S. Davis[c]

[a]*Dartmouth College, Hanover, NH 03755-8000, USA*
[b]*Department of Marine Science, University of Georgia, Athens, GA, USA*
[c]*Woods Hole Oceanographic Institution, Woods Hole, MA, USA*

Abstract

A detailed physical model of Georges Bank, including M_2 tidal rectification, realistic topography, Mellor-Yamada 2.5 mixed-layer dynamics, and time-varying wind forcing, was used to simulate plankton transport. Wind records from January 1 through March 4 of each year from 1968 through 1993 were selected to force the model. For each year, two model runs were made, one time-variant and the other using the mean wind stress for the entire period. Simulations using no wind and a 26-year climatological mean (1968–1998) also were conducted. Differences in net transport and 2-month mean currents between the vector-averaged and time-varying runs for a given year were slight. Plankton distribution in time-varying winds moved in response to transient wind events, but distributions at the end of the 60-day simulation period were remarkably similar to those from model runs using vector-averages of the same winds. Interannual differences were significant; depending on the direction of the mean wind stress, tracers were transported to several different regions on and off the bank. The use of wind-stress averages over a 2-month period is supported for models addressing transport on that time scale. Interannual variability in winter wind stress may play a major role in determining transport and subsequent recruitment of plankton on the bank. © 2000 Published by Elsevier Science Ltd.

1. Introduction

It is well known that variability in wind forcing can have a large impact on plankton dynamics through its effect on vertical mixing, but its influence on horizontal transport remains poorly understood. Davis (1982, 1984, 1987) suggested that the low observed abundance of the copepod

---

[☆] Paper published in December 2000.

[*] Corresponding author. Fax: 1-603-646-3856.

E-mail address: cvl@dartmouth.edu (C.V.W. Lewis).

Pseudocalanus on Georges Bank in February 1979 (compared with February of 1975) was due to a washout of the population by strong wind forcing. Subsequently, Lewis et al. (1994) modeled the short-term effects of strong wind forcing during early spring on the transport of bank populations. The physical model was the Semi-Spectral Primitive Equation Model (Gawarkiewicz, 1993; Haidvogel et al., 1991) applied to an idealized Georges Bank with simple topography (circular with a conical cap). This physical model was coupled to two different biological models (a stage-structured *Pseudocalanus* model and a simple food-web model) to show that steady forcing by strong winds can cause partial "washout" of populations (Lewis et al., 1994).

Recently a series of physical and biological models have been developed to study the transport and development of copepods and bivalve and fish larvae in the climatological flowfields of the Georges Bank/Gulf of Maine region (Holboke, 1998; Lough et al., 1994; Lynch and Naimie, 1993; Lynch et al., 1995, 1996, 1998; Naimie et al., 1994; Naimie, 1996; Miller et al., 1998; Ridderinkhof and Loder, 1994; Tremblay et al., 1994; Werner et al., 1993, 1996). The use of climatologically averaged wind stress provides an estimate of seasonal forcing levels (e.g. Lynch et al., 1998), but it remains unclear whether time-averaged forcing generates accurate estimates of plankton transport. More generally, these and other models of plankton transport in this region have either ignored winds or used steady wind forcing (Davis, 1984; Chen, 1992; Chen et al., 1995; Chen and Beardsley, 1995; Franks and Chen, 1996; Greenberg, 1983; Klein, 1987). It is necessary, therefore, to examine the potential importance of time-varying wind forcing on plankton transport in this region.

A brief consideration of Georges Bank reveals an area of complex interactions between topographic and oceanographic features with the potential for unexpected nonlinear effects of wind forcing. The bank is a shallow, roughly elliptical, submarine plateau lying east of Cape Cod, Massachusetts (Fig. 1). As defined by the 100-m isobath, Georges Bank is approximately 150 km wide by 280 km long, with an area of about 34,000 km². The southern half of the bank is dominated by a gradual sloping plain, extending from the 60-m isobath out to a continental slope. On the northern half, within the 60-m isobath, are a complex series of shoals and overlying sand waves that rise, in some places, to within a few meters of the surface (Twichell et al., 1987; Uchupi and Austin, 1987).

The dominant processes driving bank circulation in all seasons are density stratification, tidal rectification and wind; the strength of the contributing processes and the overall circulation vary seasonally. Detailed discussion of circulation in this region can be found elsewhere (Backus and Bourne, 1987; Butman et al., 1982; Butman and Beardsley, 1987; Loder, 1980; Loder and Wright, 1985; Loder et al., 1992).

The onset of winter, with stronger winds and cooling, causes a breakdown of thermal stratification. Intense recirculation and frontal structures, characteristic of summer conditions on Georges Bank, weaken and may be lost entirely in intense winter storms. The spatial transition from thermally stratified (deeper) to well-mixed (shallow) water that characterizes the tidal mixing front on the South Flank disappears, although a weakened version of the tidal mixing front persists on the North Flank. Density effects due to salinity gradients (highest in the Slope Water) are largely compensated for by gradients in temperature (colder over the bank crest). Temperatures on the bank in winter are uniformly low, typically averaging 4°C over much of the bank, increasing to 10°C in the shelf-slope front (Flagg, 1987).

The transport of plankton over Georges Bank is a result of the interactions of these highly variable nonlinear processes. In such a topographically and oceanographically complex regime, the
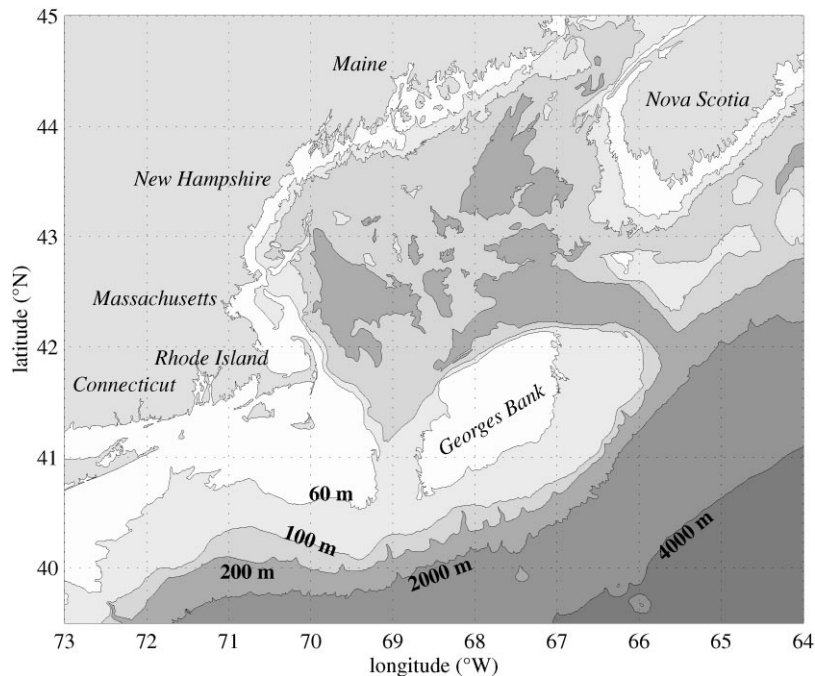
Fig. 1. Map of Georges Bank and the surrounding region. Shown are the coastline, 60, 100, 200, 2000 and 4000-m isobaths.

effect of variability in one process may involve compensating and magnifying effects of other processes driving bank circulation (Lewis et al., 1994). The objective of this paper is to examine the effects of time-varying winds and tidal forcing on transport of plankton on Georges Bank.

2. Methods

A series of numerical experiments were conducted to isolate the effects of wind forcing on the transport of plankton over Georges Bank. Transport across the boundaries of the bank and between subregions was examined. Plankton transport was modeled based on wind records from January 1 to March 4 (120 M_2 tidal cycles) of all years from 1968 to 1993 (Fig. 4 and Table 1). Within this set of 26 runs, four were selected whose forcing conditions bracket the range of variation in wind-forced processes. These simulations are intended to identify process effects rather than to simulate specific conditions and plankton distributions within a given year.

All 26 years were simulated twice; one run used time-variant wind records based on 6-h Fleet Numerical Oceanography Center (FNOC) wind data for 41°N 68°W, and the second used a constant forcing equal to the vector-averaged wind stress over the same period. A pair of runs, one using no wind and the other using the average for the January–February period of data from the years 1968–1993, were made for comparison to the annual results. Our focus is on the bank-scale response over a 2-month period; spatial variation in wind stress was neglected in these simulations.

Table 1
Mean wind magnitude and source direction for vector-averaged wind stress for 120 tidal M_2 cycles (62.3 days) starting January 1

Year	Mean (m s^{-1})	Direction (°)	τ_E (dyn cm^{-2})	τ_N (dyn cm^{-2})	STD (τ) (dyn cm^{-2})
1968	8.18	329	0.414	− 0.687	2.411
1969	8.70	15	− 0.236	− 0.877	2.978
1970	6.18	325	0.261	− 0.377	2.345
1971	4.81	298	0.246	− 0.130	1.878
1972	3.92	304	0.153	− 0.104	2.523
1973	7.87	4	− 0.055	− 0.741	3.179
1974	6.59	337	0.206	− 0.478	2.801
1975	5.34	319	0.222	− 0.260	1.496
1976	7.10	266	0.604	− 0.039	2.259
1977	7.56	302	0.583	− 0.362	2.221
1978	2.50	317	0.051	− 0.055	2.455
1979	8.07	322	0.482	− 0.616	2.798
1980	9.07	6	− 0.103	− 0.982	3.247
1981	5.59	330	0.185	− 0.326	2.432
1982	7.82	325	0.420	− 0.603	2.148
1983	7.25	24	− 0.253	− 0.577	2.266
1984	3.47	351	0.022	− 0.143	1.199
1985	7.94	317	0.513	− 0.555	1.919
1986	5.51	322	0.227	− 0.286	1.423
1987	8.30	344	0.234	− 0.793	2.588
1988	4.82	292	0.259	− 0.104	1.683
1989	5.93	331	0.207	− 0.367	2.087
1990	6.42	263	0.491	0.058	1.502
1991	4.03	294	0.177	− 0.081	1.248
1992	5.76	337	0.153	− 0.368	1.959
1993	7.84	17	− 0.217	− 0.706	2.883
Clim.	6.13	333	0.202	− 0.403	2.329

2.1. Model description

We use a version of ECOM-si (Blumberg and Mellor, 1983, 1987; Blumberg, 1993) para-meterized for Georges Bank and the Gulf of Maine region. This model has been used extensively in this region, and detailed descriptions of the model code and limitations have been published (Blumberg and Mellor, 1983, 1987; Blumberg, 1993; Chen, 1992; Chen et al., 1995). Only a summary of the salient features used in this work is presented here.

ECOM-si is designed to solve the primitive equations of fluid motion over scales of 1–100 km. The equations for momentum advection include the Boussinesq, incompressibility, hydrostatic and f-plane approximations (calculated for latitude 41°N, $f = 9.57 \times 10^{-5}\,\text{s}^{-1}$):

$$u_t + \mathbf{u} \cdot \nabla u - fv = -\frac{p_x}{\rho_0} + (K_m u_z)_z + F_u, \tag{1}$$

$$v_t + \mathbf{u} \cdot \nabla v + fu = -\frac{p_y}{\rho_0} + (K_m v_z)_z + F_v, \tag{2}$$

$$\nabla \cdot \mathbf{u} = 0, \tag{3}$$

$$p_z = -\rho_0 g, \tag{4}$$

where u, v and w are the x, y and z components of the local velocity vector, $\mathbf{u}$ (subscripts x, y, z and t denote the three spatial and one temporal derivative), p represents pressure, ρ_0 is the reference density, K_m is the vertical turbulent eddy viscosity, and F_u and F_v represent the sub-grid scale horizontal momentum diffusion terms (Blumberg and Mellor, 1987). The cases addressed here all assume an unstratified water column, approximating winter and spring conditions.

The mixing coefficients, K_m and K_H, are derived from the Mellor and Yamada second-order turbulence closure model; they are calculated from a model of the turbulent kinetic energy (q^2) and turbulent macroscale (l) as follows (Blumberg and Mellor, 1987; Chen et al., 1995; Mellor and Yamada, 1982):

$$q_t^2 + \mathbf{u} \cdot \nabla q^2 = 2\left(P_s - \frac{q^3}{B_1 l}\right) + (K_q q_z^2)_z + F_q, \tag{5}$$

$$(q^2 l)_t + \mathbf{u}.\nabla(q^2 l) = l E_1 P_s - \frac{q^3 W}{B_1} + (K_q (q^2 l)_z)_z + F_1. \tag{6}$$

P_s represents the production of turbulent kinetic energy from shear,

$$P_s = K_m(u_z^2 + v_z^2). \tag{7}$$

W represents a wall proximity function (Eqs. (9) and (11)) that limits the turbulence scale in proximity to the surface and bottom boundaries. The mixing coefficients for momentum (K_m), tracer quantities (K_H), and the two turbulence quantities (K_q), then can be calculated from the following equations:

$$K_m = lqS_m, \quad K_H = lqS_H, \quad K_q = lqS_q. \tag{8}$$

S_m, S_H and S_q are analytically derived stability functions, and E_1 and B_1 are empirically derived constants (Blumberg and Mellor, 1987; Chen et al., 1995; Mellor and Yamada, 1982). F_q and F_1 incorporate the effects of lateral diffusion of mixing energy and scales. This work assumed constant horizontal mixing ($40\,\mathrm{m^2\,s^{-1}}$) for all properties.

The surface ($z = \eta$) boundary conditions for the above equations included only the effects of wind stress (τ_w):

$$\left.\begin{aligned} &\rho_0 K_m \langle u, v \rangle_z = \tau_w \\ &w = u\eta_x + v\eta_y + \eta_t \\ &q^2 = B_1^{2/3}|\tau_w| \\ &q^2 l = 0 \end{aligned}\right\} \text{at} \quad z = \eta. \tag{9}$$

The wind stress, τ_w, is calculated from the wind vector, $\mathbf{u}_w$, as follows:

$$\tau_w = C_d |\mathbf{u}_w| \mathbf{u}_w$$

$$C_d = \begin{cases} 1.2 \times 10^{-3} & |\mathbf{u}_w| < 11\,\mathrm{m\,s^{-1}} \\ (0.49 + 0.065|\mathbf{u}_w|) \times 10^{-3} & 11\,\mathrm{m\,s^{-1}} < |\mathbf{u}_w| < 25\,\mathrm{m\,s^{-1}} \\ 2.1 \times 10^{-3} & 25\,\mathrm{m\,s^{-1}} < |\mathbf{u}_w|, \end{cases} \tag{10}$$

where $|\mathbf{u}_w|$ denotes the magnitude of the wind vector $\sqrt{u_w^2 + v_w^2}$ (Large and Pond, 1981).

The bottom boundary condition ($z = -H$) is governed only by bottom friction:

$$\left. \begin{aligned} & \rho_0 K_m \langle u, v \rangle_z = \tau_f \\ & w = -uH_x - vH_y \\ & q_2 = B_1^{2/3} |\tau_f| \\ & q^2 l = 0 \end{aligned} \right\} \text{at} \quad z = -H. \tag{11}$$

The bottom stress (τ_f) is determined from the bottom slip velocity, $\mathbf{u}_b$.

$$\tau_f = C_d |\mathbf{u}_b| \mathbf{u}_b$$

$$C_d = \max\left(\frac{\kappa}{\ln(z_b/z_0)^2}, 0.0025 \right), \tag{12}$$

where $\kappa(0.4)$ is the von Kármán constant, z_b is the thickness of the bottom layer (1.39 m in the shallowest region of the bank), and $z_0(0.001)$ is the roughness parameter (Blumberg and Mellor, 1987; Mellor and Yamada, 1982).

The above equations provide three-dimensional prognostic prediction of three velocity components, surface elevation, turbulent kinetic energy and turbulent macroscale. They also allow the prediction of transport of passively advected plankton (B):

$$B_t + \mathbf{u} \cdot \nabla B = (K_H B_z)_z + F_B + R_B. \tag{13}$$

Sub-grid scale diffusion is included using the term F_B. Reaction terms incorporating the effects of biological interactions (R_B) can be included on the right-hand side of Eq. (13), but this work discusses only the effects of physical transport (i.e. $R_B = 0$).

The equations are solved on a finite difference grid in three dimensions, with a horizontal grid scale of approximately 5 km and 15 sigma levels vertically. The grid domain represents the topography of the Gulf of Maine and Georges Bank (Fig. 2). A staggered Arakawa C grid is used; velocity components are indexed to the edges of the grid cell, and all other components are referenced to the midpoint of the cell. An orthogonal curvilinear grid is used in the horizontal, yielding a model domain with better coverage in the area of interest. The vertical structure is resolved using a sigma coordinate system, with $\sigma = (z - \eta)/(H + \eta)$. The overall domain contains 140 elements in the along-shelf direction, 100 across the shelf, and 16 points in the vertical (Fig. 2); the grid includes dry land points at which solutions are not calculated.

The model domain and associated grid includes all of the Gulf of Maine and Georges Bank region, extending over 100 km south of the 100 m isobath at all points. The coastal boundaries to the north include smoothed realistic bathymetry for the Gulf of Maine region and are closed at
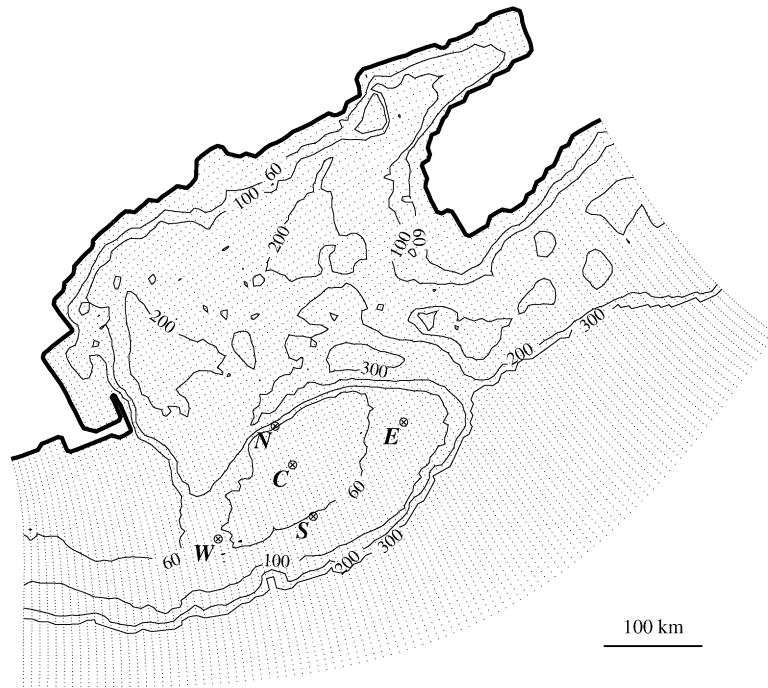
Fig. 2. Model grid and topography. Location of model grid points are indicated by small dots; coastline is shown in bold. The full time and depth structure of velocity are recorded at locations indicated by an $\otimes$ and associated station letter (N, S, E and W).

coastal points with no-flux boundaries. The eastern and western boundaries (to the south of Nova Scotia and Cape Cod) are open, as is the southern boundary into deep water. A 15-point sponge is used at the western boundary to absorb gravity wave energy propagating toward that boundary, while a 10-point sponge is used at both the southern and eastern boundaries. The grid was extended by 30 points on the western boundary to compensate for numerical difficulties in that region that had limited the solution to $\sim$ 20 days. This extension consisted of a 30-point repetition of the topography at that boundary and successfully stabilized the model for the full 60-day runs shown here. Only the behavior of interior points in the neighborhood of Georges Bank is discussed here, as the selected boundary conditions exclude some important processes (e.g. warm-core rings, Gulf Stream meanders, and riverine buoyancy fluxes).

The semi-implicit feature of the model allowed for longer time step at this resolution than would a fully explicit model. The model uses an implicit scheme in the vertical direction and a semi-implicit solution in the horizontal direction for the barotropic mode; the semi-implicit scheme uses the free surface gradient to solve the velocity divergence in the continuity equation implicitly (Blumberg, 1993; Casulli, 1990; Chen et al., 1995). The solutions discussed below use a time step of 465.75 s; this choice yields 96 time steps per M_2 tidal cycle.

The vertical profile of the horizontal components of current (u and v) was recorded every time step at five locations over the bank (Denoted N, E, S, W, and C in Fig. 2). In this discussion, *Residual* velocities are defined as the time average of velocity over one tidal cycle (12.42 h).

Depth-averaged current values are averages of the horizontal vector components of current over the entire water column.

2.2. Initial conditions and forcing

Initial conditions for the physical parameters approximate the winter condition on Georges Bank after stratification has been broken down by mixing and cooling. During this period the circulation is dominated by an underlying tidal signal with time-varying wind-forced flow. The physical model was initialized with quiescent, unstratified water with sea-surface height uniformly equal to zero throughout the domain. The model forcing included two processes: a tidal signal generated by free-surface forcing at the open boundaries and time-varying wind-stress imposed uniformly over the entire surface.

In order to remove initial transient behaviors, the model was allowed to equilibrate for 10 tidal cycles ($\sim$ 5 days); the tidal signal was linearly increased to full strength over the course of one tidal cycle while the wind forcing was linearly increased (to the initial value for the given run) over 10 tidal cycles. Linear increasing initial wind forcing was chosen to provide a wind forced component to the flow field at the start of the run. The tidal component achieved a stable periodic pattern within 2–3 tidal cycles. Equilibration was rapid, and no instabilities were detected in any of the 2-month simulations described here.

The biological model was initialized, after the physical model had spun up, with a set of tracer fields ("plankton") whose distributions were selected based on two criteria. First, the initial plankton distributions completely covered the bank (within the 100-m isobath), allowing calculation of total bank losses; second, the subdivision isolates bank subregions thought to be ecologically and oceanographically distinct. Nine patches were used to describe the distribution of plankton originating at the bottom in nine different subregions of the bank (Fig. 3). These fields were seeded after 10 tidal cycles. Plankton were initialized at the bottom, with the integral of the depth distribution (areal density) at each point equal to $1.0 \, \text{m}^{-2}$, i.e. all the plankton were placed in the grid point closest to the bottom, with a volumetric density inversely proportional to depth. This is consistent with a scenario in which larvae are produced at an equal rate by benthic organisms in all regions. Vertical flux off the bottom was relatively rapid due to vertical mixing. The depth distribution of plankton was relatively homogeneous after two tidal cycles.

Wind forcing records from 26 years (1968–1993) were compared, using FNOC wind data for latitude 41°N and longitude 68°W (Bakun, 1973, Table 1). Wind records from the period between January 1 and March 4 were used (Fig. 8). For each year, the model was run twice, comparing the effects of the time-varying FNOC record and the time-invariant vector-averaged wind stress of the entire period.

These choices allow estimation of the effect of two types of wind variability on plankton transport. First, the comparison between model runs using a 2-month vector-averaged wind-stress and time-varying model (wind variability at 6-h intervals) addresses the effects of such high-frequency variability and the necessity of its inclusion in future modeling of transport on bimonthly time scales. Second, the choice of scenarios (mean and variable winds for 26 individual years, no wind and climatology) effectively covers the likely range of observed bimonthly wind-stress averages (Fig. 4). These simulations are designed to assess the magnitude of the processes studied; a hindcast of actual conditions during the selected years would require a much more detailed study
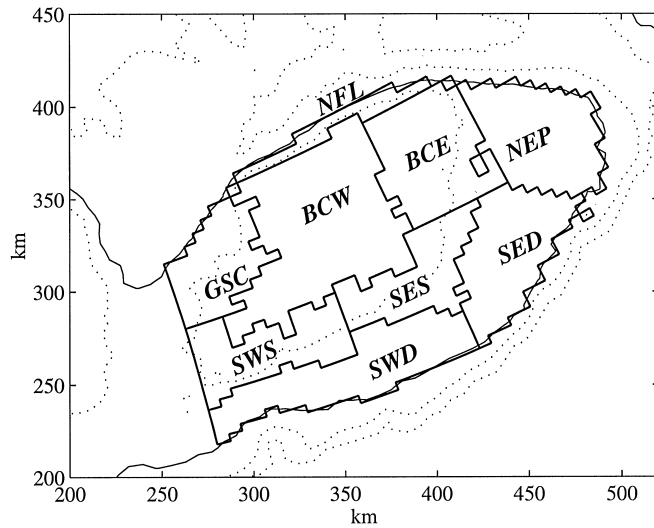
Fig. 3. Initial plankton patch distributions. Each patch is indicated by three-letter codes and delineated by solid lines.
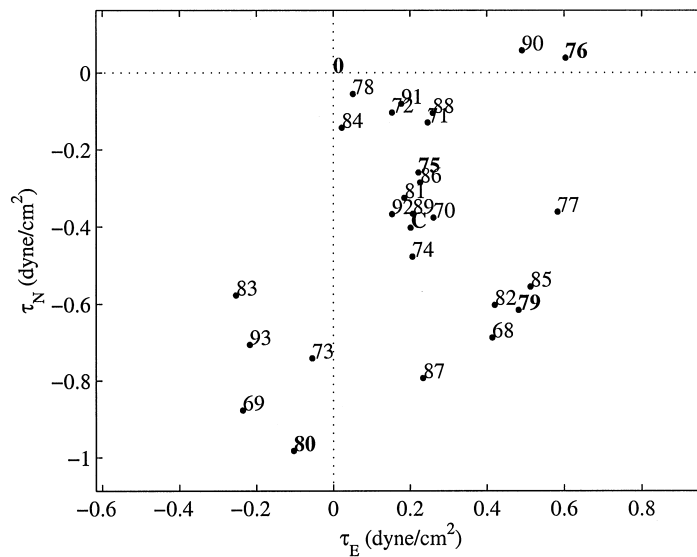
Fig. 4. Distribution of bimonthly average wind stress for January and February, 1968–1993. Also shown is the climatological average (C).

of the effects of stratification and boundary forcings than has been proven feasible at these time and space scales.

The model boundaries were forced with a sinusoidal surface gravity wave with an amplitude of 0.50 m at the lunar semi-diurnal period (M_2: 12.42 h) at the southern and western boundaries and an amplitude increasing from 0.50 to 0.76 m at the eastern boundary. All boundaries were forced in
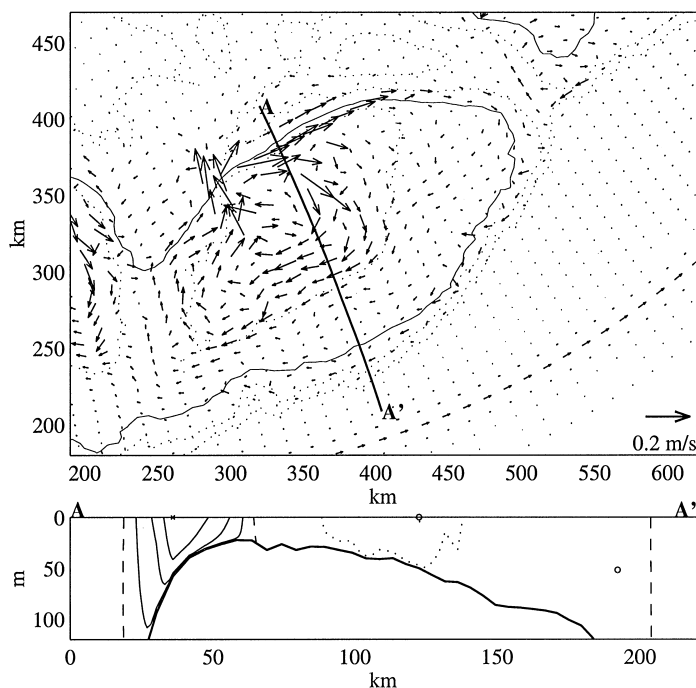
Fig. 5. (Top) Depth-averaged tidal residual currents for a run with no wind. Bold line indicates 100 m isobath. (Bottom) Contour plot of $0.05 \, \mathrm{m \, s^{-1}}$ isopleths of velocity (normal to section shown in top panel). Positive contours (into page) are shown solid, zero contour is dashed, negative contours dotted. Local velocity maxima are denoted by an "x", local minima by an "o".

phase. These time-dependent surface elevation boundary conditions are very similar to observations over the bank (Brown, 1987).

3. Results

The model provided information regarding the currents in response to the tidal and wind forcing as well as an estimate of the distributions of transported plankton patches. Little difference was found in comparison of transport and long-term average velocities for simulations using average and time-varying winds for a given year; however, results differed markedly between years.

3.1. Currents

When subject only to tidal forcing without wind ($\tau_w = 0$), the modeled tidal residual circulation closely resembled previous models and observational data (Butman et al., 1987; Greenberg, 1983; Flagg, 1987; Lynch and Naimie, 1993; Tremblay et al., 1994; Naimie et al., 1994) in pattern and magnitude. The depth-averaged residual currents in the Georges Bank region (Fig. 5, Table 2) show a strong ($0.17 \, \mathrm{m \, s^{-1}}$) Northern Flank jet (produced by tidal rectification along the steep

Table 2
Mean and standard deviation of *on-* and *around-bank* velocity (cm s^{-1}) for time varying (TV) and average wind stress (Ave.) wind forcing for 1975, 1976, 1979 and 1980 at four peripheral locations on Georges Bank (described in Fig. 2: E = Northeast Peak, S = South Flank, W = Great South Channel and N = North Flank). Positive values indicate flow onto the bank and in the direction of the prevailing anticyclonic gyre

	E	S	W	N
On-Bank				
No wind	− 0.9	0.0	1.1	2.6
Climatology	− 0.2	− 0.2	0.3	2.9
1975 TV	− 0.4 ± 2.6	− 0.3 ± 1.7	0.7 ± 4.4	2.9 ± 1.8
1975 Av.	− 0.4	− 0.3	0.7	3.1
1976 TV	− 0.9 ± 4.9	− 1.1 ± 3.3	2.3 ± 8.2	3.7 ± 2.8
1976 Av.	− 1.0	− 1.0	2.2	3.7
1979 TV	0.3 ± 4.4	− 0.7 ± 2.7	0.0 ± 6.8	3.5 ± 3.4
1979 Av.	0.2	− 0.6	0.1	3.5
1980 TV	0.9 ± 6.0	0.4 ± 3.9	− 1.7 ± 10.6	2.5 ± 3.5
1980 Av.	0.9	0.4	− 1.9	2.3
Around-Bank				
No wind	2.3	4.3	1.6	17.3
Climatology	2.4	5.5	1.1	15.4
1975 TV	2.5 ± 1.3	5.0 ± 4.1	1.2 ± 2.3	15.8 ± 4.6
1975 Av.	2.5	5.0	1.1	16.0
1976 TV	3.2 ± 2.1	3.7 ± 7.2	1.2 ± 3.8	16.5 ± 7.0
1976 Av.	3.1	3.7	0.8	16.9
1979 TV	2.7 ± 2.1	5.9 ± 6.9	0.6 ± 4.0	13.7 ± 9.0
1979 Av.	2.6	6.0	0.6	14.2
1980 TV	1.7 ± 3.7	7.9 ± 9.5	1.1 ± 3.9	12.9 ± 8.7
1980 Av.	1.7	7.8	1.1	13.1

topography; Loder, 1980), with weak recirculation on the South Flank and strongest recirculation inside the 60-m isobath. Currents on the Northeast Peak were diffuse and undirected, as has been noted previously (Butman et al., 1987; Flag, 1987), although other modeling work predicts a much stronger jet along the North Flank onto the Northeast Peak (Naimie, 1996; Naimie et al., 1994), likely due to both the inclusion of stratification effects and the large-scale climatological mean pressure field imposed on the latter model.

The circulation in the model runs with climatological wind forcing bore a strong qualitative resemblance to the circulation with only tidal forcing (Figs. 5 and 6). These runs equilibrated (within 5 days) to a periodic flow field in which temporal variation was solely due to the M$_2$ tide. The residual currents after initialization showed no noticeable trends in current speed or direction for the entire 60 days.

The effect of time-varying wind forcing on the distribution of depth-averaged on bank and around-bank velocity was to cause high levels of variation in the residual currents (Fig. 7) without markedly altering the mean velocity (four cases: 1975, 1976, 1979 and 1980 are considered in Table 2 and Fig. 8). A very close relationship exists between the mean currents in the vector-averaged and
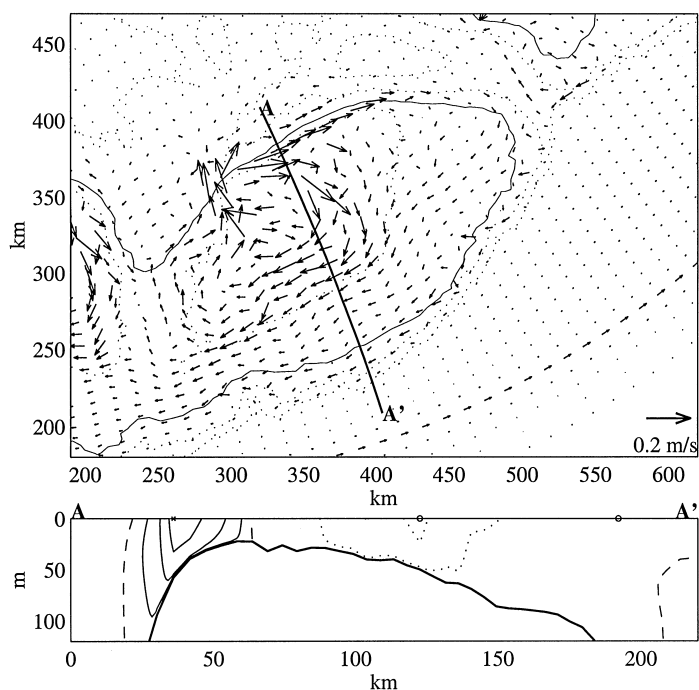
Fig. 6. Residual currents for simulations using climatological mean wind forcing. (Top) Depth-averaged tidal residual currents. Bold line indicates 100-m isobath. (Bottom) Contour plot of $0.5 \, \mathrm{m \, s^{-1}}$ isopleths of velocity (normal to section shown in top panel). Labeling conventions as Fig. 5.

time-varying case, implying that, on long time scales, much of the variability in wind forcing is accounted for by the vector-averaging of wind stress, even in this relatively complex flow environment. However, the addition of wind variability introduces a level of current variability that is often of the same magnitude as the mean.

In most cases, mean wind stress from the north and west resulted in the addition of a south-westerly flow component. On the North Flank (N), this tended to inhibit the around-bank flow and increase flow onto the bank, while it had the opposite effect on South Flank (S). The Northeast Peak (E) had a slight increase in around- and on-bank flow, while the Great South Channel (W) had decreases in on- and around-bank flow as a result of wind forcing. Despite the minor differences in mean residual velocity between the vector-averaged and time-varying cases, there were still a number of notable short-term wind events in each year that drove sharp transient responses in modeled currents (Fig. 8).

In the time-varying 1975 run there were very few major wind events of sufficient strength to strongly affect the North Flank jet at station N (Fig. 8). Depth-averaged on-bank (across isobath) flow at station N never increased above $10 \, \mathrm{cm \, s^{-1}}$, and the around-bank (along isobath) residual flow at this station was weakly reversed only once (day 10). Wind events produced little variation in the direction and magnitude of the depth-averaged, tidal residual flow. The depth-averaged residual flow at station N consistently shows a strong North Flank jet only occasionally altered by
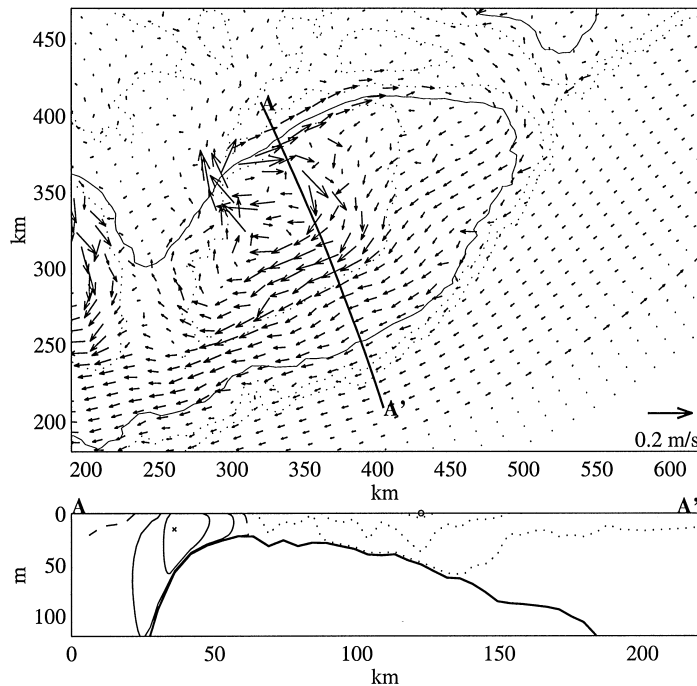
Fig. 7. Residual currents for simulations using 1980 mean wind forcing. (Top) Depth-averaged tidal residual currents. Bold line indicates 100 m isobath. (Bottom) Contour plot of 0.5 m s^{-1} isopleths of velocity (normal to section shown in top panel). Labeling conventions as Fig. 5.

episodic wind forcing. Overall, events in the 1975 variable-wind forced flows failed to penetrate deeply into the water column.

In 1976 there was consistent on-bank flow across the North Flank, consistent with the fact that Ekman transport for the average west winds would be expected to drive on-bank flows (Fig. 8). The around bank flow was never entirely disrupted; in this 2-month period the wind-driven circulation was never strong enough to cause a reversal of the North Flank Jet. A few small storm events do stand out, but the variability in this record is fairly slight when compared to the 1979 and 1980.

By contrast, 1979 variable winds drove residual on-bank flows at station N up to 20 cm s^{-1}, with many periods where on-bank flow exceeded 5 cm s^{-1} (Fig. 8). In this simulation there were four separate wind events during which the depth-averaged flow at this station was reversed, at one point reaching 16 cm s^{-1} in the counterclockwise direction (day 37). Storm events repeatedly penetrated deep into the water column on the bank, causing residual surface velocities to reach 0.5 m s^{-1} over the central and southern flank of Georges Bank where the surface tidal-residual component was typically less than 0.1 m s^{-1}. The flow in the North Flank jet (station N) was completely disrupted several times. On day 22, the around-bank surface residual component briefly exceeded 0.4 m s^{-1}.

In 1980, the record shows long calm periods disrupted by severe storms during days 5–20 and around day 38. These two periods show very strong wind events that entirely reverse the
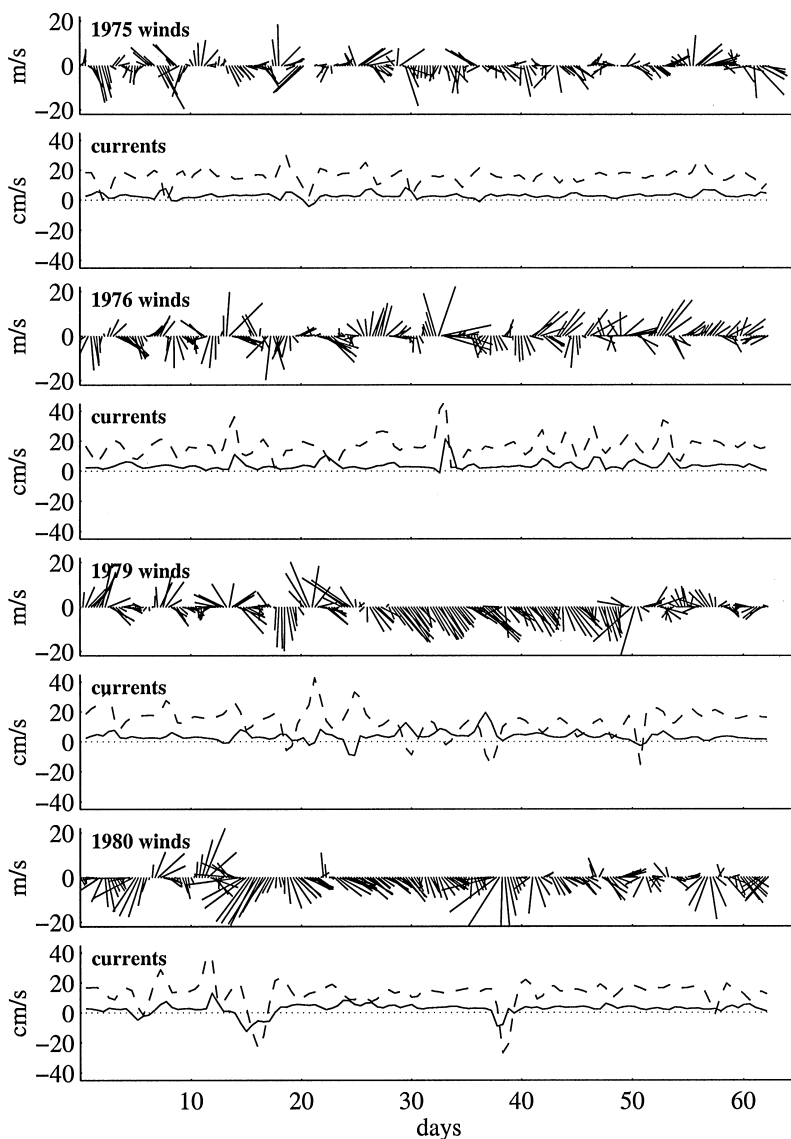
Fig. 8. Wind forcing and resulting depth-averaged residual currents on the North Flank for four runs with time-varying forcing. Shown are four years bracketing the range of observed variability: 1975 (near climatology), 1976 (strong westerly), 1979 (strong northwesterly) and 1980 (strong northerly). Dashed lines are around-bank currents (positive clockwise) and solid lines are on-bank (positive onshore).

depth-averaged flow on the north flank, driving a strong off-bank flow. Although these reversals are comparatively brief, they have a marked effect on the 2-month mean currents (Table 2) and the transport and fate of tracers over the entire bank (Fig. 10). As will be seen, the effect of these comparatively short reversals is captured by the long-term transport as well.
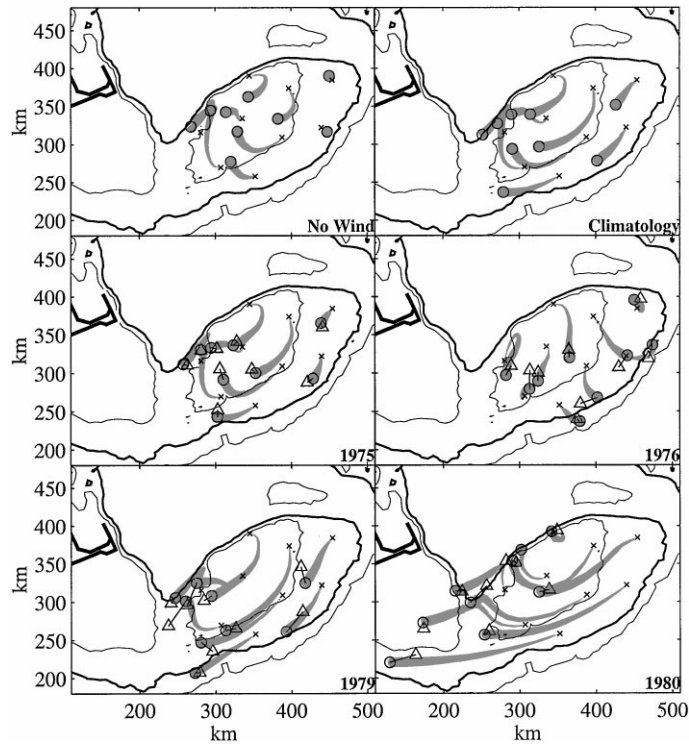
Fig. 9. Track of the center of mass for each plankton patch for each model run. Tracks originate at locations marked with a +; location of the centroid after 62 days of invariant time-averaged winds is denoted by an ∘. For comparison, the location of the center of mass of each patch under time-varying winds is shown by a linked △.

3.2. Plankton transport

The interannual differences observed in the velocity field also were noted in comparisons of transport of plankton under the various wind forcing regimes. The results of the plankton transport models are best summarized by the time courses of the center of mass of each of the modeled plankton patches (Fig. 9, patch locations described in Fig. 3) and retention of plankton within the 100 m isobath and within source regions (Figs. 10 and 11). The time course of plankton transport can be approximated by tracking the center of mass of each plankton patch (Fig. 9). The comparison of four different years transport from each of the three regions of the bank indicates that interannual differences are significant whereas the effect of high-frequency wind variability has only a slight effect on the fate of transported plankton is general.

Using vector-averaged winds causes the location of the centroid to proceed smoothly around the bank, while the time course of patch transport under variable winds is much more random (not shown). However, the net effect of the winds in either case is surprisingly similar. Comparing the final locations of the center of mass in the time-varying and average cases (Fig. 9) shows that, over the 2-month period, the centroids are typically less than 10 km apart. Transport for different years
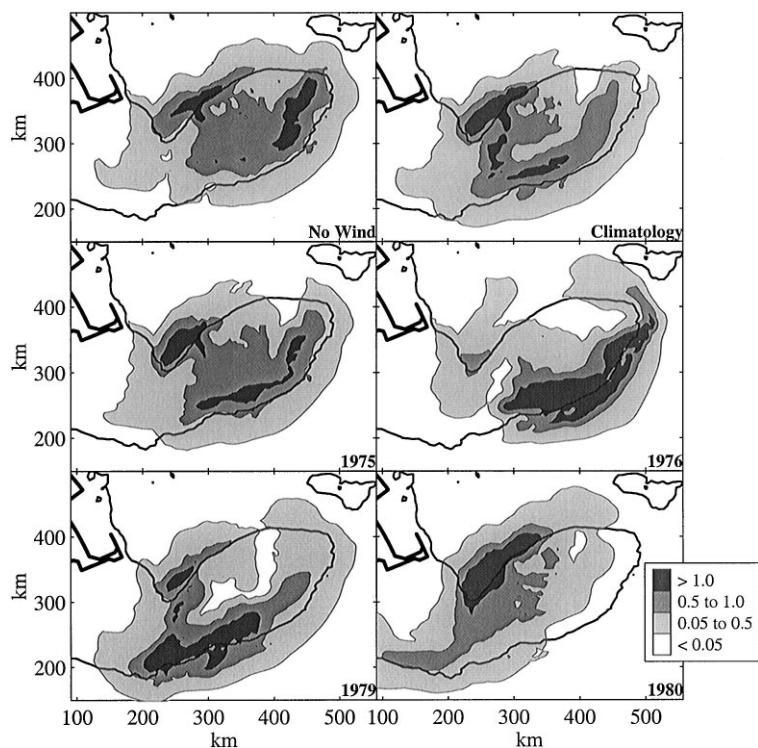
Fig. 10. Plankton distribution for 1975, 1976, 1979 and 1980 after 60 days of transport for all plankton originating within the 100-m isobath on bank.

shows a much greater separation; for example, results for 1975 closely resemble the climatology, whereas the strong north winds of 1980 drove plankton well west and north of the bank (Fig. 10).

In the no-wind, climatological and 1975 cases, the individual plankton patches are largely retained over the bank with the introduction of wind, causing an increased transport to the southwest. By comparison, the extreme cases represented by 1976, 1979 and 1980 show a marked wind-driven response. The 1976 winds, strongly to the east, drove the various patches to the south, consistent with Ekman transport. The addition of an Ekman component also helps explain the results of 1979 and 1980, where strong winds to the south and southeast cause a marked increase in the displacement to the southwest.

Another picture of the effects of wind transport can be seen by examining the final distribution of plankton from the bank (Fig. 10). The no-wind case tends to show the least net displacement, with plankton remaining centered largely over the bank. In the 1975 and climatological cases, the patches were carried farther south and west, but still largely centered over the bank. By comparison, the final distribution of plankton in the three extreme cases saw the bulk of the patch carried off the South Flank (1976), to the far southeast corner of the bank (1979) or blown into the north end of the Great South Channel (1980). Similar variability was seen between other years modeled; for example, results for 1980 were similar to those from 1969, 1973, 1993 and 1983, and results from 1990 and 1976 were very similar.
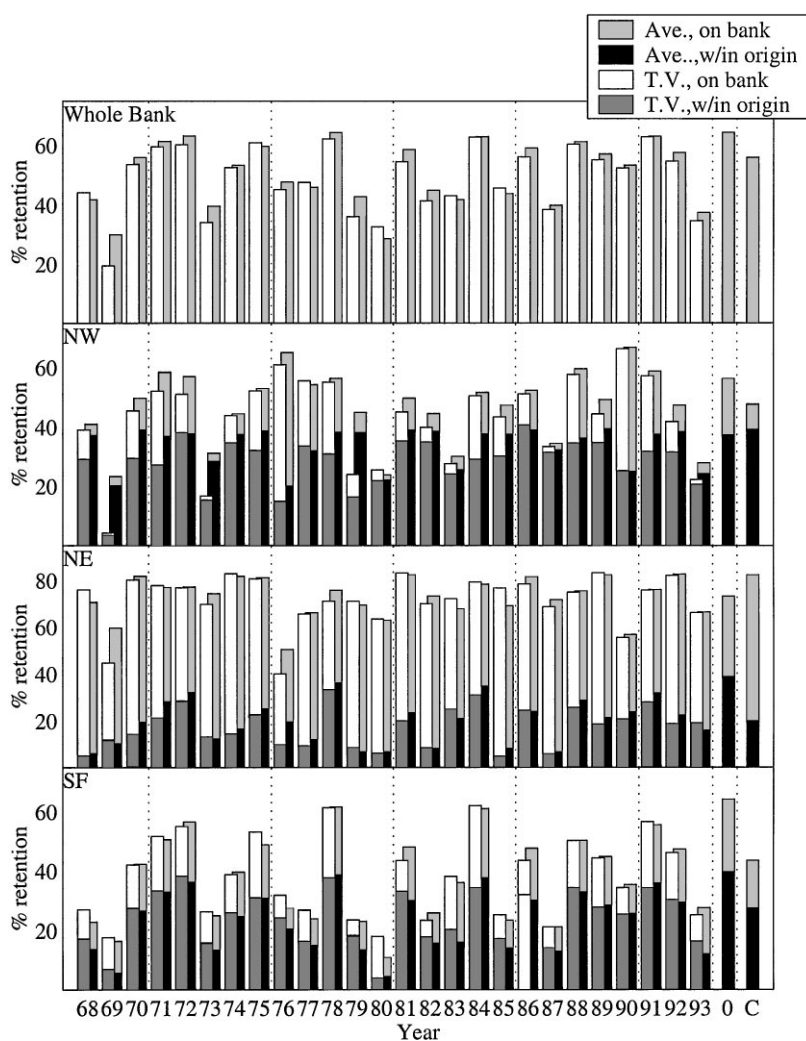
Fig. 11. Percent of the tracer remaining within source region (darker bars) and within the perimeter of the bank (upper and lower portion combined) for wind-stress averaged (Ave.), time-varying wind (TV), Climatological (C) and no-wind (0) runs.

3.3. Plankton retention and loss

Retention of plankton from each region varied widely between years; retention of plankton from the whole bank varied from a low of $\sim 20\%$ in 1969 to a high of $\sim 65\%$ in 1972 and 1978. However, there was very close agreement between the calculated retention of each field in simulations using time-varying and vector-averaged winds for a given year (Fig. 11). In most cases, the retention calculated for simulations using vector-averaged winds is within 10% of that using time-varying winds.

The interaction of wind forcing with transport from the regions to the west and north of the bank (NFL, GSC, and BCW) showed few trends. Typically, approximately 40% of the plankton remained within the source region while another 10–20% was swept south onto the rest of the bank. Off-bank losses from this region tended to occur to the west and north. An extreme example is 1969, where, in the time-varying case, strong winds from the north left less than 5% of the plankton from this region on the bank.

Those plankton originating over the eastern portion of the bank crest and the Northeast Peak (BCE and NEP) were consistently retained on the bank. Retention within the source region was low; these plankton were washed south and west, seeding much of the South Flank. This area served as a source population for much of the rest of the bank, feeding into other regions but supplying less to itself.

Plankton from the southern and western portions of the bank (regions SES, SWS, SED, and SWD) tended to experience the greatest losses in most cases and showed the most variability between years. As seen in Fig. 9, plankton from this region tended to sweep south and west along the shelf toward Nantucket shoals. Retention was highest in years with low winds; northwest winds common in the winter tended to quickly drive plankton from this region off the south flank. Retention that does occur tends to result from a weak recirculation in the western portions of the bank and through the Great South Channel.

Overall the retention of plankton over a 2-month period reflects the interannual variability, but is surprisingly insensitive to high-frequency variability. Even in an extreme case, such as 1980 where a pair of storms sharply biased the 2-month average, the transport is accurately represented by the average winds.

4. Discussion

The simulations highlighted interactions between tidal circulation and wind forcing that have important consequences for the retention and recruitment of plankton over Georges Bank. Winter winds have the potential to dominate the tidal circulation and drive large portions of developing plankton populations off the bank. In the 26-year period considered here, the winter winds were predominately to the east and south, with a 2-month vector-averaged wind-stress ranging from 2.5 to $9.1\,\mathrm{m\,s^{-1}}$, with losses of plankton ranging from 40 to 80%.

Use of a time-invariant average wind stress had little effect on the long-term (2 month) mean of currents at a given location or on net transport of plankton over the entire averaging period. Wind events at time scales much shorter than the 2-month averaging period had only a transient impact on circulation and transport; the net effect of the short period events on bimonthly transport was minimal. Differences in the average wind stress between years drove noticeable variation in the transport of plankton over a 2-month period.

With respect to the technical requirements of modeling circulation over Georges Bank, it appears that time-varying wind forcing has little effect on the overall circulation and calculated transport of modeled plankton over a 2-month period. The generally high variability in the wind, several times the magnitude of the mean, is markedly reduced in the currents, where the variability is less than the mean. While there exist nonlinear effects (e.g. mixing, residence time in various

locations), the effects of wind variation on bimonthly transport appear to be well captured by long-term wind-stress average.

A closer analysis of the time-varying wind runs indicates that the time course of transport is highly erratic compared to the average wind runs (cf. Fig. 8). This higher frequency variability in transport may have significant effects on nonlinear interactions such bloom dynamics, sediment and nutrient resuspension, and trophic dynamics. The effect of wind-event timing is not addressed; for example, if the storms observed in the 1980 wind record had occurred 2 weeks earlier or 2 weeks later, the effect on developing plankton populations might have been significantly different. Early storms might drive fecund adults onto the bank from the Gulf of Maine early in the season, giving the bank population a "jump-start" on the spring bloom; conversely, a later storm could sweep a developing cohort off the bank, effectively restarting the development of the bank population.

The model identified several general trends in the circulation around Georges Bank that may have significant effects on the retention of planktonic communities on the bank. The results highlighted three features of the bank circulation that may be important for the retention and survival of planktonic organisms. First, they indicate that the northern end of the Great South Channel is a consistent site of retention and recirculation, even in the face of fairly strong winds. Second, retention of plankton over the southern flank of the bank is low in most years; it was sharply reduced by strong winds from the west and northwest. Even the weakest of winter wind forcing is sufficient to drive plankton from the deeper portions of the south flank off the bank and into deep water. Third, this work identifies those regions where transport and loss rates are sensitive to wind forcing, specifically the southern and western regions of the bank, and regions where the on-bank retention was highest, the Northeast Peak.

These results suggest that the Northeast Peak is the most "secure" region for developing populations wishing to remain on the bank, while the western and southern portions of the bank may seed onto regions of the Middle Atlantic Bight but are less important for the development of Georges Bank populations.

Several basic conclusions can be drawn concerning the impact of winds on Georges Bank ecosystems. The results imply that strong north and northwest winds have the capability to markedly increase losses of plankton off the South Flank of the bank. Models using realistic wind forcing generally give transport and retention results differing only slightly from models forced with vector averages of the same winds. In addition, populations on the Northeast Peak were identified as a source region for much of the South Flank, while plankton from the southern and western portions of the bank tended to be driven into the Great South Channel or lost entirely from the bank.

The link between simple advective model processes and the full trophic dynamics underlying cod and haddock recruitment requires extensive further study; also needed is a more complete analysis of the physical mechanisms underlying these transport patterns; including gulf-scale response and along-shelf pressure variability. However, this work indicates that the planktonic food source for larval cod may be swept from the bank by extended storms, potentially exposing newly hatched larvae to starvation and extra predation risks in an depleted prey environment. Additionally, the Northeast Peak spawning pattern for cod is identified as a region least susceptible to advective losses from winter storms. This work strongly indicates that understanding of interannual variability in recruitment requires consideration of the variation in the advective effects of wind-forced transport.

Acknowledgements

References

Backus, R.H., Bourne, D.W. (Eds.), 1987. Georges Bank. MIT Press, Cambridge, MA.

Bakun, A., 1973. Coastal upwelling indices, west coast of North America, 1946–71. Technical Report NOAA-TR-NMFS-SSRF 671, National Oceanic and Atmospheric Administration.

Blumberg, A.F., 1993. A primer for ECOM-si. Technical Report, Hydroqual, Mahwah, NJ.

Blumberg, A.F., Mellor, G.L., 1983. Diagnostic and prognostic numerical circulation studies of the South Atlantic Bight. Journal of Geophysical Research 88 (C8), 4579–4592.

Blumberg, A.F., Mellor, G.L., 1987. A description of a three-dimensional coastal ocean circulation model. In: Heaps, N.S. (Ed.), Three-Dimensional Coastal Ocean Models. American Geophysical Union, Washington, DC, pp. 1–16.

Brown, B., 1987. The fisheries resources. In: Backus, R.H., Bourne, D.W. (Eds.), Georges Bank. MIT Press, Cambridge, MA, pp. 480–493.

Butman, B., Beardsley, R.C., 1987. Long-term observations on the southern flank of Georges Bank, Part I: a description of the seasonal cycle of currents, temperature, stratification and wind stress. Journal of Physical Oceanography 17, 367–384.

Butman, B., Beardsley, R.C., Magnell, B., Frye, D., Vermersh, J.A., Schlitz, R., Limeburner, R., Wright, W.R., Noble, M., 1982. Recent observations of the mean circulation on Georges Bank. Journal o Physical Oceanography 12, 559–591.

Butman, B., Loder, J.W., Beardsley, R.C., 1987. The seasonal mean circulation: observation and theory. In: Backus, R.H., Bourne, D.W. (Eds.), Georges Bank. MIT Press, Cambridge, MA, pp. 125–138.

Casulli, V., 1990. Semi-implicit finite difference methods for the two-dimensional shallow water equations. Journal Computational Physics 86, 56–74.

Chen, C., 1992. Variability of currents in Great South Channel and over Georges Bank: observation and modeling. Ph.D. thesis, Woods Hole Oceanographic Institution Joint Program, Massachusetts Institute of Technology.

Chen, C., Beardsley, R.C., 1995. A numerical study of stratified tidal rectification over finite-amplitude banks, Part I: symmetric banks. Journal of Physical Oceanography 25, 2090–2110.

Chen, C., Beardsley, R.C., Limeburner, R., 1995. A numerical study of stratified tidal rectification over finite-amplitude banks, Part II: Georges Bank. Journal of Physical Oceanography 25, 2111–2128.

Davis, C., 1982. Processes controlling zooplankton abundance on Georges Bank. Ph.D. Thesis, Boston University Marine Program, Woods Hole, MA.

Davis, C.S., 1984. Interaction of a copepod population with the mean circulation on Georges Bank. Journal of Marine Research 42, 31–40.

Davis, C.S., 1987. Zooplankton life cycles. In: Backus, R.H., Bourne, D.W. (Eds.), Georges Bank. MIT Press, Cambridge, MA, pp. 256–267.

Flagg, C., 1987. Hydrographic structure and variability. In: Backus, R.H., Bourne, D.W. (Eds.), Georges Bank. MIT Press, Cambridge, MA, pp. 108–124.

Franks, P.J.S., Chen, C., 1996. Plankton production in tidal fronts: a model of Georges Bank in summer. Journal of Marine Research 54, 631–651.

Gawarkiewicz, G., 1993. Steady wind forcing of a density front over a circular bank. Journal of Marine Research 51, 109–134.

Greenberg, D., 1983. Modeling the mean barotropic circulation in the Bay of Fundy and the Gulf of Maine. Journal of Physical Oceanography 13, 886–904.

Haidvogel, D., Wilkin, J., Young, R., 1991. A semi-spectral primitive equation ocean circulation model using vertical sigma and orthogonal curvilinear coordinates. Journal of Computational Physics 94, 151–185.

Holboke, M.J., 1998. Variability of maine coastal current under spring conditions. Ph.D. Thesis, Dartmouth College RN845.

Klein, P., 1987. A simulation of some physical and biologic interactions. In: Backus, R.H., Bourne, D.W. (Eds.), Georges Bank. MIT Press, Cambridge, MA, pp. 395–402, RN844.

Large, W.G., Pond, S., 1981. Open ocean momentum flux measurements in moderate to strong winds. Journal of Physical Oceanography 11, 324–336.

Lewis, C.V.W., 1997. Biological–physical interactions on Georges Bank: plankton transport and population dynamics of the Ocean Quahog, Arctica islandica. Ph.D., Woods Hole Oceanographic Institution Joint Program, Massachusetts Institute of Technology.

Lewis, C.V.W., Davis, C.S., Gawarkiewicz, G., 1994. Wind forced biological-physical interactions on an isolated offshore bank. Deep-Sea Research II 41 (1), 51–73.

Loder, J., 1980. Topographic rectification of tidal currents on the sides of Georges Bank. Journal of Physical Oceanography 10, 1399–1416.

Loder, J.W., Brickman, D., Horne, E.P., 1992. Detailed structure of currents and hydrography on the northern side of Georges Bank. Journal of Geophysical Research 97 (C9), 14331–14351.

Loder, J.W., Wright, D.G., 1985. Tidal rectification and frontal circulation on the sides of Georges Bank. Journal of Marine Research 43, 581–604.

Lough, R.G., Smith, W.G., Werner, F.E., Loder, J.W., Page. F.H., Hannah, C.G., Naimie, C.E., Perry, R.I., Sinclair, M., Lynch, D.R., 1994. Influence of wind-driven advection on interannual variability in cod egg and larval distributions on Georges Bank: 1982 vs 1985. ICES Marine Science Symposium, Vol. 198, pp. 356–378.

Lynch, D.R., Gentleman, W.C., McGillicuddy, D., Davis, C.S., 1998. Biophysical simulations of Calanus finamrchicus population dynamics in the Gulf of Maine. Marine Ecology Progress Series 169, 189–210.

Lynch, D.R., Ip, J.C., Naimie, C.E., Werner, F.E., 1995. Convergence studies of tidally-rectified circulation on Georges Bank. In: Lynch, D.R., Davies, A.M. (Eds.), Quantitative Skill Assessment for Coastal Ocean Models, Coastal and Estuarine Studies, Vol. 48, American Geophysical Union, Washington, DC.

Lynch, D.R., Ip, J.T.C., Naimie, C.E., Werner, F.E., 1996. Comprehensive coastal circulation model with application to the Gulf of Maine. Continental Shelf Research 16 (7), 875–906.

Lynch, D.R., Naimie, C.E., 1993. The M2 tide and its residual on the outer banks of the Gulf of Maine. Journal of Physical Oceanography 23, 2222–2253.

Mellor, G.L., Yamada, T., 1982. Development of a turbulence closure model for geophysical fluid problems. Reviews of Geophysics and Space Physics 20 (4), 851–875.

Miller, C.B., Lynch, D.R., Carlotti, F., Gentleman, W., Lewis, C., 1998. Coupling of individual-based population dynamical models for stocks of Calanus finmarchicus with numerical models of flow in the region of Georges Bank. Fisheries Oceanography 7 (3/4), 219–234, RN813.

Naimie, C.E., 1996. Georges Bank residual circulation during weak and strong stratification periods: prognostic numerical model results. Journal of Geophysical Research 101 (C3), 6469–6486.

Naimie, C.E., Loder, J.W., Lynch, D.R., 1994. Seasonal variation of the three-dimensional residual circulation on Georges Bank. Journal of Geophysical Research 99 (C8), 15967–15989.

Ridderinkhof, H., Loder, J.W., 1994. Lagrangian characterization of circulation over submarine banks with applications to the outer Gulf of Maine. Journal of Physical Oceanography 24, 1184–1200.

Tremblay, M.J., Loder, J.W., Werner, F.E., Naimie, C.E., Page, F.H., Sinclair, M.M., 1994. Drift of sea scallop larvae Placopecten magellanicus on Georges Bank: a model study of the roles of mean advection, larval behavior and larval origin. Deep-Sea Research II 41 (1), 7–49.

Twichell, D.C., Butman, B., Lewis, R.S., 1987. Shallow structure, surficial geology, and the processes currently shaping the bank. In: Backus, R.H., Bourne, D.W. (Eds.), George Bank. MIT Press, Cambridge, MA, pp. 31–37.

Uchupi, E., Austin, J.A., 1987. Morphology. In: Backus, R.H., Bourne, D.W. (Eds.), George Bank. MIT Press, Cambridge, MA, pp. 25–30.

Werner, F.E., Page, F.H., Lynch, D.R., Loder, J.W., Lough, R.G., Perry, R.I., Greenberg, D.A., Sinclair, M.M., 1993. Influences of mean advection and simple behavior on the distribution of cod and haddock early life stages on Georges Bank. Fisheries Oceanography 2 (2), 43–64.

Werner, F.E., Perry, R.I., Lough, R.G., Naimie, C.E., 1996. Trophodynamic and advective influences on Georges Bank larval cod and haddock. Deep-Sea Research II 43 (7–8), 1793–1822.